Solitary waves dynamic for Davydov α-helical protein model: Effects of localized and periodic inhomogeneities

R. Y. Ondoua[1,2,*] and D. Belobo Belobo[2,3,4,†]

[1]*Department of Physics, Faculty of Science, University of Douala, P.O. Box 24157, Douala, Cameroon*

[2]*Laboratory of Biophysics, Department of Physics, Faculty of Science, University of Yaounde I, P.O. Box 812, Yaounde, Cameroon*

[3]*African Centre for Advanced Studies, P.O. Box 4477, Yaounde, Cameroon*

[4]*Department of Mathematics and Physical Sciences, National Advanced School of Engineering of Yaounde, University of Yaounde I, P.O. Box 8390, Yaounde, Cameroon*

(Received 29 June 2020; revised 6 October 2020; accepted 27 November 2020; published 11 December 2020)

We describe the dynamic of excitons through single inhomogeneous α-helical proteins with off-diagonal and diagonal couplings. Inhomogeneities considered are either localized or periodic. Intensive numerical simulations carried show stable structures and allow us to single out important features of excitons dynamic. In the absence of inhomogeneities, the interplay between off-diagonal and diagonal couplings leads to two distinct types of solitary waves. Bright solitary waves correspond to an off-diagonal coupling constant lower than a critical diagonal coupling constant, while dark solitary waves are obtained in the opposite case. Inclusion of inhomogeneities profoundly affects the profiles, amplitudes, and energies transported by the waves. For relatively small strength of inhomogeneities, only the profiles of the waves significantly change, the other properties remaining almost unchanged. Large strength inhomogeneities sensitively twist the profiles and increase amplitudes and energies of the waves. Our study suggests that small strength inhomogeneities allow a coherent transport of energy and the biological functions remain unchanged, but large strengths of inhomogeneities affect the biological functioning of the α-helical protein chains. Hence, large strengths of inhomogeneities may amplify the energy of the molecule and could be used to treat some diseases.

DOI: 10.1103/PhysRevE.102.062414

I. INTRODUCTION

Proteins are an important class of biological macromolecules present in all living organisms. There are a myriad of proteins that play different biological functions such as hormones, antibodies, transporters, and antibiotics, to name a few. The task of each protein is intimately related to its structure, the latter being classified as primary, secondary, tertiary, and quaternary. The secondary structure is important as it allows us to explain many activities of the protein. It refers to highly regular local substructures. Two main types of secondary structure, the α-helix and the β strand or β sheet were suggested in 1951 by Pauling, Corey, and Branson [1]. It has been shown that α-helices are more stable, robust to mutations and designable than β-strands in natural proteins [2]. Designing functional all α-helices proteins is likely to be easier than designing proteins with both helices and strands as suggested by a recent experiment [3].

A biological role for vibrational excited states was first proposed by McClare in connection with a possible crisis in bioenergy [4]. Davydov applied Mcclare's proposal to α-helix protein molecules to explain the conformational changes responsible for muscle contraction induced by the energy donating reaction of the adenosine-triphosphate (ATP) hydrolysis [5,6]. He suggested that the amide-I energy could stay localized through the nonlinear interactions of the vibrational excitation with the deformation in the protein's structure caused by the presence of the excitation. The excitation and the deformation cancel each other and form a soliton (localized wave that lasts very long keeping its original main properties). In the strict sense, solitons are localized exact solutions of integrable nonlinear partial differential equations that collide elastically. Solitary waves are localized solutions of non integrable partial differential equations. The bioenergy may be transported along the protein molecules in virtue of the motion of the soliton. This mechanism may be described classically as follow. The vibrational energy of the amide-I ($C = O$) stretching oscillators that is localized on the helix chains acts through a phonon coupling effect and deforms the structure of the amino acid residue, the deformation of the amino acid residues reacts again through a phonon coupling. The outcome of the latter couplings is to trap the amide-I vibrational quanta and prevent its dispersion, hence forming a soliton through this process. This effect is called self-trapping of the amide-I vibrational quantum (or exciton). Davydov's first main assignment was to point out a specific vibrational band that is found in proteins and that is ideal for the storage and propagation of energy. His second main contribution to the field of bioenergy was to realize that the amide-I energy depends on the strength of the hydrogen bond that may exist between the oxygen of one peptide group and the nitrogen of another [7–11]. Thus, Davydov took into account the coupling between the amide-I vibrations (intramolecular excitations or excitons) and deformations of amino acid residues (or

*Corresponding author: yanickondouar@yahoo.com

†belobodidier@acas-yde.org

acoustic phonons) to model the dynamic of α-helix proteins. To understand the significance of Davydov's solitons through the relevant biochemical problem, we note the following: (i) biological energy is released in units of 0.42 eV [11,12] by the hydrolysis of adenosine triphosphate (ATP) to adenosine diphosphate (ADP); (ii) a basic biological resonance unit is the amide-I bond ("$C = O$") which has a quantum of energy [a quantum of excitation (zero-point vibrational energy) in the amide-I bond] of 0.205 eV [9,11]. Most importantly, the amide-I bond is found in every peptide group of every protein. This universality of amide-I bonds in proteins led to the idea that these bonds might be pivotal in the storage as well as in the transport of the biological energy released from the hydrolysis of ATP. Spines in α-helix are good examples of soft molecular chains as required by the Davydov's model. The original Davydov's model considers only on channel or spine and further assumes that excitations are moved along the chain by dipole-dipole interactions among amide-I bonds. The continuous approximation was used to transform the relevant discrete equations of motion to a continuous nonlinear Schrödinger equation. It is well known that the continuous nonlinear Schrödinger equation sustains both single solitons and multisoliton solutions [13]. As an alternative to the original Davydov's soliton, Takeno proposed the concept of vibron solitons [14]. Unlike vibron solitons that result from a nonlinear coupling of vibrons with lattice vibrations, Davydov's solitons find their applications to excitons with transfer by exchange interactions. Simple models consider only one strand of α-helix, whereas more complete modelings suggest the existence of at least three spines for a better energy transport. This has been the main focus of the works in Refs. [15–17], where the molecule was pictured as a set of three hydrogen bonding spines [18–21]. For the purpose of clarity, we focus in this paper on the propagation of a vibration, presumably amide-I, along a single spine in an α-helical protein.

In real life, proteins are interacting with many other molecules. The presence of such other organisms like drugs, carcinogens, mutants and dyes in specific sites of the α-helical protein sequence may alter the structure of proteins, hereby inducing defects called inhomogeneities. Defects or inhomogeneities change the localized structure of the α-helix. These changes cause the soliton to slow down or stop disrupting the energy and information transfer through the protein. Solitons important parameters, namely the energy, amplitude, velocity, position and phase are expected to be altered by the presence of inhomogeneities in the system. The effects of mass inhomogeneities on the energy transfer through solitons motion in α-helical proteins were studied by Simo [22] who showed that such a system is governed by a standard elliptic type equation. He concluded that in the case of heavy mass-induced impurities, oscillatory motion may be accounted by dn-type solitons. The effect of nonlinear inhomogeneities in the form of modified exchange interactions between sites was addressed in terms of solitons under perturbation in Ref. [23]. Applying the sine-cosine method, Merlin and Latha proved that the presence of inhomogeneities causes soliton splitting and hence a disorder in the protein molecular system [23]. In Ref. [24], a model accounting for inhomogeneous α-helical proteins including excitations, dipole-dipole interactions between nearest and next-nearest neighbors and interspine coupling was introduced. The authors found that above a critical value of the inhomogeneity, the energy is no longer transported with good efficiency due to fluctuations in the soliton. Therewith, it has been shown that localized inhomogeneities do not alter the velocity nor the amplitude of the soliton during propagation [25]. Recently, the dynamical behaviors of solitonic interactions and the influence of the protein inhomogeneity on shape-changing collisions of solitons were discussed by direct numerical simulations of a three-coupled variable coefficients nonlinear Schrödinger equation [26]. Nevertheless, most of these works used analytical methods to describe the physical effects of the inhomogeneities in biological molecules. However, instabilities may be embedded into analytical solutions leading to their destructions such that they may not be observed in real experiments. Such limitations are circumvented by comparing analytical results to numerical ones that are more reliable. Therefore, in this paper we study numerically the effects of inhomogeneities in an intra spine based on the kundu's model [27] which advantages are the presence of both diagonal and off-diagonal couplings in α-helical protein chains. The presence of the off-diagonal coupling allows to detect two types of nonlinear solitary waves that may be propagate through the protein chain. We recall that, the Davydov's model used in the current work remains valid at temperatures lower than 220 K [28]. The recent experiment carried by Pang *et al.* [28] confirmed the existence of bright solitons as energy carriers in protein chains (the study used the collagen molecule as a sample of α-helix protein chain) at 320 K suggests that under similar experimental conditions, our analysis that considers the Davydov's model may be valid at temperatures lower than 220 K.

The rest of this paper is organized as follows. in Sec. II, we describe the model and derive the equation of motion. Numerical simulations are performed in Sec. III, both in the absence and presence of inhomogeneities. This allows us to underline the effects of inhomogeneities of different types on the dynamic of the exciton. Section IV is devoted to concluding remarks.

II. THE MODEL

We consider a model described by Kundu [27] and include a site-dependent inhomogeneity f_n. This inhomogeneity arises in the α-helix chain by means of a defect or a drug molecule in the energy site of the amide-I bond. The inhomogeneity considered here is a site-dependent one which modifies the interaction exchange between neighboring sites, characterizes dipole-dipole interactions along the hydrogen bonding spine. In this work, the inhomogeneity is introduced phenomenologically. The Hamiltonian associated with the model which is the standard Su-Schriffer-Heeger hamiltonian $H_{\rm SSH}$ can be written as [27,29–31]

$$\begin{aligned} H_{\rm SSH} = & \frac{1}{2}\sum_n \left[\frac{P_n^2}{M} + K(\beta_n - \beta_{n+1})^2\right] \\ & + \sum_n \{[Jf_n - \alpha(\beta_n - \beta_{n+1})](a_{n+1}^\dagger a_n + a_n^\dagger a_{n+1})\} \\ & - \chi \sum_n (\beta_{n+1} - \beta_{n-1}) a_n^\dagger a_n. \end{aligned} \tag{1}$$

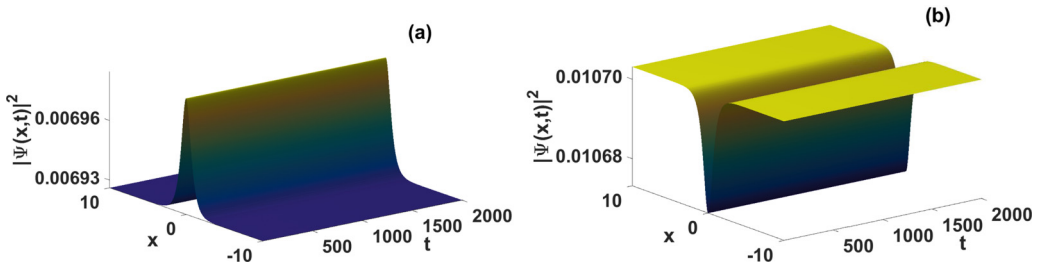

FIG. 1. Spatiotemporal evolutions of densities of solitary waves. (a) $\alpha = 9.92 \times 10^{-12}$ N and $\chi = 61.76 \times 10^{-12}$ N ($\alpha < \chi$). (b) $\alpha = 78.92 \times 10^{-12}$ N and $\chi = 61.76 \times 10^{-12}$ N ($\alpha > \chi$). Interplay between off-diagonal coupling (α) and diagonal coupling (χ) affects the profile of solutions. Other parameters are $k = 1.8$, $\rho = 1.0$, $K = 19.36$ N, $J = 15.47 \times 10^{-23}$ J, and $M = 1.9 \times 10^{-25}$ Kg.

In Eq. (1), β_n represents the displacement of the nth $H - N - C = O$ unit from its equilibrium position and a_n ($a_n^\dagger$) is the annihilation (creation) operator of a spinless vibron [a quantum of excitation (zero-point vibrational energy) in the amide-I bond] in a Wannier-type orbital localized at site n. J accounts for the dipole-dipole coupling of amide-I vibration while α is the off-diagonal coupling. P_n stands for the conjugate momentum of the vibrational coordinate β_n and M represents the reduced mass of one peptide unit. K is the elastic coefficient of the hydrogen bonds while χ accounts for the diagonal coupling constant [17].

Let us define the dynamical equations that govern the system. To this end, we consider state vectors that we define as tensor products of a normalized one-exciton state and a coherent phonon state accounted by $|\Phi(t)\rangle$ with the form

$$|\Phi(t)\rangle = |\phi_e\rangle \otimes |\phi_{\rm ph}\rangle. \tag{2}$$

In Eq. (2), $|\phi_e\rangle$ and $|\phi_{\rm ph}\rangle$ represent the exciton state and the phonon state, respectively, and are given by

$$|\phi_e\rangle = \sum_n \varphi_n(t) a_n^\dagger |0\rangle_e, \tag{3}$$

$$|\phi_{\rm ph}\rangle = \exp\left[\sum_q (\alpha_q \varphi_q^* - \alpha_q^* \varphi_q)\right] |0\rangle_{\rm ph}, \tag{4}$$

where $|0\rangle_e$ is the ground state of the exciton, while $|0\rangle_{\rm ph}$ is the ground state of the phonon in the space $\xi_{\rm ph}$ such that for all q, $\varphi_q|0\rangle_{\rm ph} = 0$. The star (*) in Eq. (4) and below stands for complex conjugation. It is well known that in the Davydov's model, the Hamiltonian is a sum of independent oscillators of pulsation w_q related to α_q by the equation

$$\alpha_q = \sqrt{\frac{M\omega_q}{2\hbar}} u_q + i\sqrt{\frac{1}{2\hbar M\omega_q}} \pi_q, \tag{5}$$

u_q and π_q being real numbers. The functions φ_q and φ_q^* are related to the system parameters by the following equation:

$$\frac{i}{\hbar} \sum_n (u_n P_n - \pi_n \beta_n) = \sum_q (\alpha_q \varphi_q^* - \alpha_q^* \varphi_q). \tag{6}$$

Assuming that the expectation values of $\beta_n(t)$ and $P_n(t)$ are $u_n(t)$ and $\pi_n(t)$, respectively, the probability of founding one quantum of excitation at the site n reads

$$|\langle 0|_1 \cdots \langle 0|_{n-1} \langle 0|_n \langle 0|_{n+1} \cdots \langle 0|_N |\phi_e\rangle|^2 = |\varphi_n|^2. \tag{7}$$

Considering that state vectors are normalized to unity leads to the condition

$$\sum_n |\varphi_n|^2 = 1. \tag{8}$$

Application of the Ehrenfest theorem for the operators β_n and P_n along with the time-dependent Schrödinger equation

$$\frac{d}{dt}\langle\phi_e|\langle\phi_{\rm ph}|\,\beta_n\,|\phi_e\rangle|\phi_{\rm ph}\rangle = \frac{1}{i\hbar}\langle\Phi(t)|[\beta_n, H_{\rm SSH}]|\Phi(t)\rangle, \tag{9}$$

$$\frac{d}{dt}\langle\phi_e|\langle\phi_{\rm ph}|\,P_n\,|\phi_e\rangle|\phi_{\rm ph}\rangle = \frac{1}{i\hbar}\langle\Phi(t)|[P_n, H_{\rm SSH}]|\Phi(t)\rangle, \tag{10}$$

$$i\hbar\frac{d}{dt}|\Phi\rangle = H_{\rm SSH}|\Phi\rangle, \tag{11}$$

yield the following coupled equations of motion

$$\begin{aligned} i\hbar\frac{d}{dt}\varphi_n(t) = {} & J(\varphi_{n+1}f_n + \varphi_{n-1}f_{n-1}) + \alpha(\beta_{n+1} - \beta_n)\varphi_{n+1} \\ & + \alpha(\beta_n - \beta_{n-1})\varphi_{n-1} - \chi(\beta_{n+1} - \beta_{n-1})\varphi_n, \end{aligned} \tag{12a}$$

$$\begin{aligned} M\frac{d^2}{dt^2}\beta_n(t) = {} & K(\beta_{n+1} + \beta_{n-1} - 2\beta_n) + \alpha(\varphi_{n+1}^*\varphi_n + \varphi_n^*\varphi_{n+1}) \\ & - \alpha(\varphi_n^*\varphi_{n-1} + \varphi_{n-1}^*\varphi_n) - \chi(|\varphi_{n+1}|^2 - |\varphi_{n-1}|^2). \end{aligned} \tag{12b}$$

When the function φ_n and β_n change smoothly over one bound of the chain, the continuum approximation may be applied [6]. This approximation is valid for long wavelengths at the low temperature limit. The continuum limit offers the advantage of being more tractable for analysis and allow in some special cases to get analytical solutions. Hence, we replace the discrete functions $\varphi_n(t)$, $\beta_n(t)$, $f_n(t)$ by their continuous counterparts $\varphi(x,t)$, $\beta(x,t)$, $f(x,t)$, respectively, with $x = n\epsilon$ where $\epsilon = 4.5$ Å [7] is the lattice parameter which is nothing else but the distance between two consecutive peptide bonds. Using Taylor series expansions $\varphi_{n\pm1} = \varphi \pm \epsilon\varphi_x + \frac{\epsilon^2}{2}\varphi_{xx} \pm \ldots$, $\beta_{n\pm1} = \beta \pm \epsilon\beta_x + \frac{\epsilon^2}{2}\beta_{xx} \pm \ldots$, $f_{n\pm1} = f \pm \epsilon f_x + \frac{\epsilon^2}{2} f_{xx} \pm \ldots$, where the suffix x represents the partial derivative with respect to x, Eqs. (12) become

$$\begin{aligned} i\hbar\varphi_t = {} & J\left[2f\varphi - \epsilon f_x\varphi + \frac{\epsilon^2}{2}(f_{xx}\varphi + 2f_x\varphi_x + 2f\varphi_{xx})\right] \\ & -2(\alpha + \chi)\epsilon\beta_x\varphi, \end{aligned} \tag{13a}$$

$$M\beta_{tt} = \frac{d}{dx}[K\epsilon^2\beta_x + 2\epsilon(\alpha - \chi)|\varphi|^2]. \tag{13b}$$

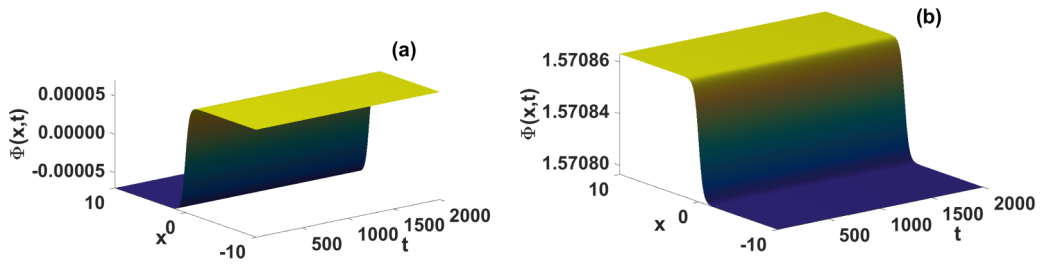

FIG. 2. Phase profile change due to interplay between off-diagonal and diagonal couplings. α. (a) $\alpha = 9.92 \times 10^{-12}$ N and $\chi = 61.76 \times 10^{-12}$ N ($\alpha < \chi$). (b) $\alpha = 78.92 \times 10^{-12}$ N and $\chi = 61.76 \times 10^{-12}$ N ($\alpha > \chi$). Other parameters as described in the caption of Fig. 1.

We consider traveling wave solutions of Eq. (13b) as excitations that propagate along the chain with velocity v, i.e.,

$$\beta(x,t) = q(x - vt), \qquad \xi = x - vt. \tag{14}$$

Inserting Eq. (14) into Eq. (13b) gives after a few algebra and return to the original variables x and t,

$$\epsilon\beta_x = -2\rho(\alpha - \chi) \mid \varphi(x,t) \mid^2, \tag{15}$$

with $\rho = \frac{1}{K(1-z^2)}$, $z = \frac{v}{v_0}$ and $v_0 = \epsilon(\frac{K}{M})^{\frac{1}{2}}$ is the longitudinal sound velocity in the chain [23]. Substituting Eq. (15) into Eq. (13a) and using the transformations $\varphi(x,t) \to u(\xi)$ and $u(\xi) \to \Psi(x,t)$, one derives the continuous equation of motion

$$i\hbar\Psi_t + \beta_0\Psi_{xx} + 2\beta_1|\Psi|^2\Psi + \beta_2\Psi + \beta_3\Psi_x = 0. \tag{16}$$

Equation (16) describes the dynamics of inhomogeneous α-helical proteins in the continuum limit, which is a perturbed nonlinear Schrödinger equation. Parameters in Eq. (16) are given by $\beta_0 = -J\epsilon^2 f$, $\beta_1 = 2\rho(\chi^2 - \alpha^2)$, $\beta_2 = -J(2f - \epsilon f_x + \frac{\epsilon^2}{2} f_{xx})$, $\beta_3 = -J\epsilon^2 f_x$. The set of parameters used to describe amide-I modes and the relationship to vibronic energy transport are defined as [17,32,33] $K = 19.36$ N/m, $\chi = 61.76 \times 10^{-12}$ N, $J = 15.47 \times 10^{-23}$ J, and $M = 1.9 \times 10^{-25}$ Kg. The value of α will be discussed throughout the analysis. Equation (16) has been derived in Ref. [24] for which the authors considered biquadratic, cubic and periodic inhomogeneities and analytically studied their effects on the dynamics of a bright solitary wave.

III. NUMERICAL ANALYSIS AND SOLITONIC SOLUTIONS

It is significant to note that numerical methods play an important role, since there is often no analytical solution for nonlinear partial differential equations used to model many phenomena in physics, biophysics especially proteins dynamics. Moreover, in the few cases where analytical solutions are available, imperfections embedded in the medium may destabilized them. It is therefore necessary to check the stability of analytical solutions as only stable solutions may be observed in experiments. The stability analysis of solutions is fully addressed by means of direct numerical integrations of the underlying nonlinear partial differential equations. Equation (16) is a derivative nonlinear Schrödinger model quite difficult to solve analytically, especially when spatial inhomogeneities are taken into account. It has been integrated numerically using the fourth-order Runge-Kutta computational scheme [36]. The spatial grid is $[-10, 10]$ with 512 points and spatial resolution $dx = 0.0391$. The time step is taken as $\Delta t = 2.33 \times 10^{-11}$. We used the F-expansion method [34,35] to find an approximate analytical expression of the solution of Eq. (16) at initial time. The solution used as initial condition for numerical simulations in almost all cases is the hyperbolic function $\Psi_0(x,0) = \sqrt{-\frac{1}{12\beta_1}(2\beta_2 - k^2\beta_0)} - \frac{k}{2}\sqrt{\frac{\beta_0}{\beta_1}}[\tanh(kx) + i\cosh^{-1}(kx)]$ (k is arbitrary real constant), is evolved up to 2000 Δt which correspond to 46.6 ns. To better understand the effects of inhomogeneities, we first considered the ideal situation where there is no inhomogeneity. In all simulations, a small amount of initial random perturbation is added to unveil any instabilities embedded in solutions. The height of the random perturbation is 0.001 that of the maximum amplitude of the initial condition.

A. Solitary waves without inhomogeneity

One advantage of the above initial condition is that it takes different profiles as the shape of the inhomogeneity changes. As we consider approximate solutions, the localized ones are solitary waves in a broader sense. In this part, there is no

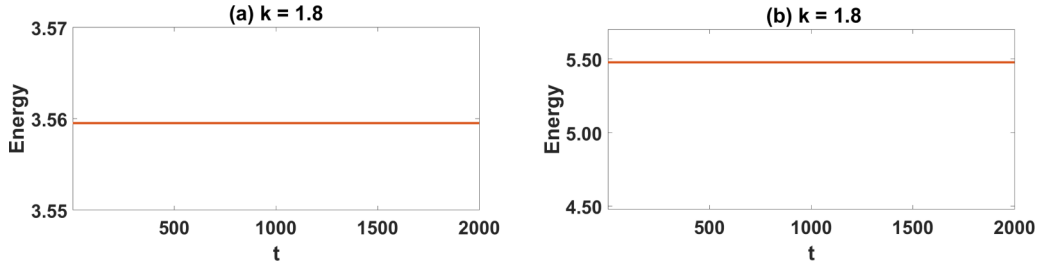

FIG. 3. Energy of the dark solitary wave is slightly greater than energy of the bright solitary wave. (a) $\alpha = 9.92 \times 10^{-12}$ N and $\chi = 61.76 \times 10^{-12}$ N ($\alpha < \chi$). (b) $\alpha = 78.92 \times 10^{-12}$ N and $\chi = 61.76 \times 10^{-12}$ N ($\alpha > \chi$). Other parameters as described in the caption of Fig. 1.

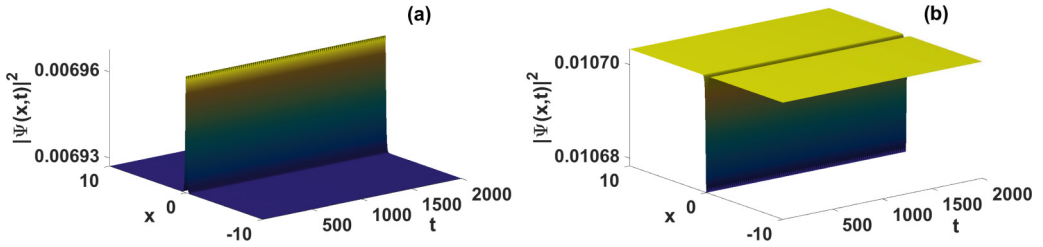

FIG. 4. Waves widths shrink due to large values of k. (a) $\alpha = 9.92 \times 10^{-12}$ N and $\chi = 61.76 \times 10^{-12}$ N ($\alpha < \chi$). (b) $\alpha = 78.92 \times 10^{-12}$ N and $\chi = 61.76 \times 10^{-12}$ N ($\alpha > \chi$). Other parameters as described in the caption of Fig. 1.

inhomogeneity, i.e., $f(x) = 1$. The above hyperbolic initial condition is inserted in the numerical code at $t = 0$. The spatiotemporal evolutions are plotted in Fig. 1. When $\alpha < \chi$ we obtain a bright solitary wave [Fig. 1(a)] while a dark solitary wave corresponds to $\alpha > \chi$ [Fig. 1(b)]. This means that the interplay between the off-diagonal coupling constant (α) and the diagonal coupling constant (χ) deeply affects the shape of the exciton dynamic propagating through the α-helical chains. In experiments, it is possible to choose the shape of the exciton-phonon coupling by adjusting the values of α and χ. Furthermore, the initial conditions in Fig. 1 persist without destruction though the insertion of small initial random perturbation. This confirms that the bright and dark solitary waves of Fig. 1 are stable, hence may be observed in real experiments. The experimental observation of solitons either bright or dark ones in α-helix protein chains may be done by measuring the infrared spectrum of absorption and Raman scattering of the protein under investigation and by identifying the presence of some specific bands that account for the presence the solitons as in Refs. [28,37,38]. Especially in Ref. [28], a bright soliton has been observed using the method in Ref. [38]. Recently, bright solitary waves were predicted in α-helical proteins for small values of α by means of the modulational instability mechanism [17,21]. Unlike the works in Refs. [17,21] where no close form analytical solutions were provided, we propose here an analytical solution at initial time to describe the dynamic of the exciton through the proteins. The numerical stability of the phases of the bright [Fig. 2(a)] and the dark [Fig. 2(b)] solitary waves, in addition to densities stability in Fig. 1, suggests that our initial condition remains valid for long time behavior. Hence, our hyperbolic initial condition is a good candidate for theoretically modeling the dynamic of exciton in α-helical protein chains. A parallel between Figs. 3(a) and 3(b) shows that the energy of the dark solitary wave is substantially greater than that of the bright solitary wave. Hence, when the off-diagonal coupling constant is larger than the diagonal coupling constant, the energy propagating through the α-helical protein is larger. Another striking feature of k is that it deeply alters the widths of the solutions which decrease with increasing values of k. This behavior is confirmed by a comparison between Fig. 4 ($k = 15$) and Fig. 1 ($k = 1.8$). In the following, we show that inhomogeneities profoundly affect the dynamic of the exciton in single α-helical proteins.

B. Effects of inhomogeneities on α-helical proteins

In this part of the work, we analyze the influence of inhomogeneities of different forms on the dynamics of the exciton through protein chains. Direct numerical integrations of

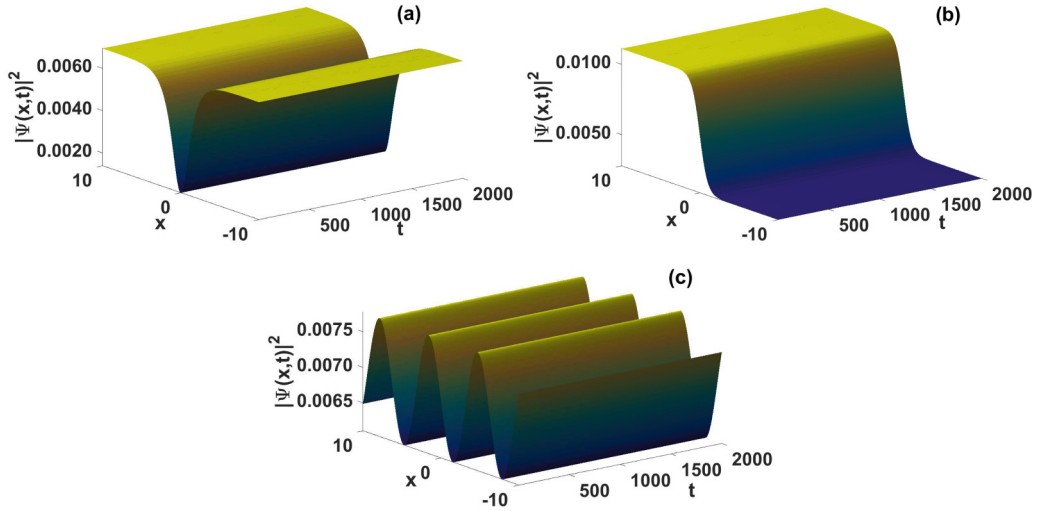

FIG. 5. Inhomogeneities profoundly change the profiles of solutions as compared to the unperturbed case of Fig. 1(a). Each type of inhomogeneity has its specific impact on the profile of solutions. (a) Localized inhomogeneity $f(x) = 1 + P_0 \cosh^{-1}(x)$, $P_0 = -0.8$, (b) localized inhomogeneity $f(x) = 1 + R \tanh(x), R = 0.6$, (c) periodic inhomogeneity $f(x) = 1 + P_1 \sin(x), P_1 = 0.12, \alpha = 9.92 \times 10^{-12}$ N, and $\chi = 61.76 \times 10^{-12}$ N($\alpha < \chi$). Other parameters as described in the caption of Fig. 1.

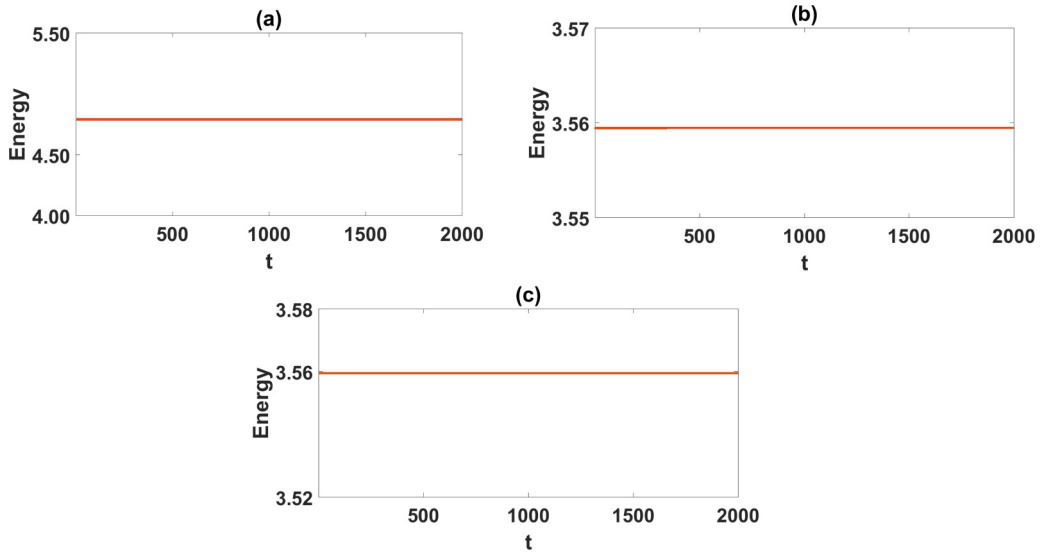

FIG. 6. The energy of the wave slightly decreases with inhomogeneities. (a) Localized inhomogeneity $f(x) = 1 + P_0 \cosh^{-1}(x)$, $P_0 = -0.8$, (b) localized inhomogeneity $f(x) = 1 + R\tanh(x)$, $R = 0.6$, (c) periodic inhomogeneity $f(x) = 1 + P_1 \sin(x)$, $P_1 = 0.12$. $\alpha = 9.92 \times 10^{-12}$ N, and $\chi = 61.76 \times 10^{-12}$ N ($\alpha < \chi$). Other parameters as described in the caption of Fig. 1.

Eq. (16) are carried by inserting spatial dependent expressions of the function $f(x)$ which accounts for inhomogeneities. A localized inhomogeneity may correspond to the intercalation of a compound between neighboring atoms similar to the insertion of a drug molecule which the α-helical protein has to unwind, leading to the distortion of the helix at the intercalated sites. Periodic inhomogeneities stand for periodic repetitions of defects or molecules along the α-helical protein chain [24].

We start by considering the case where $\alpha < \chi$. For the localized inhomogeneity of the the form $f(x) = 1 + P_0 \cosh^{-1}(x)$ with $k = 1.8$ and $P_0 = -0.8$, Fig. 5(a) shows a stable dark solitary wave solution rather different from its bright solitary wave counterpart obtained in Fig. 1(a) in the absence of the inhomogeneity ([$f(x) = 1$]. Using the localized inhomogeneity of the form $f(x) = 1 + R\tanh(x)$ with $R = 0.6$ yields a stable kink like profile solution displayed in Fig. 5(b). Generally, solutions of the kink type materialize the deformations of a biological helix and not the transport of energy in this one. Nevertheless, it is not excluded to consider biological implications related to the transport of energy in α-helical proteins by means kink type solutions. The same type of solutions were obtained by Yakada *et al.* through the generalized Riccati equation mapping method for the modeling of signal transmission through an electrical lattice [39]. A periodic inhomogeneity $f(x) = 1 + P_1 \sin(x)$ with $P_1 = 0.12$ has been used to obtain a periodic solution presented in Fig. 5(c). Comparing Figs. 5(a)–5(c) with Fig. 1(a) shows that inhomogeneities deeply alter the profile of the spatiotemporal evolution of the exciton through the α-helical protein chain. A result similar to the one in Fig. 5(c) was predicted through analytical calculations in Ref. [23]. It was suggested that such periodic oscillations are likely to induce

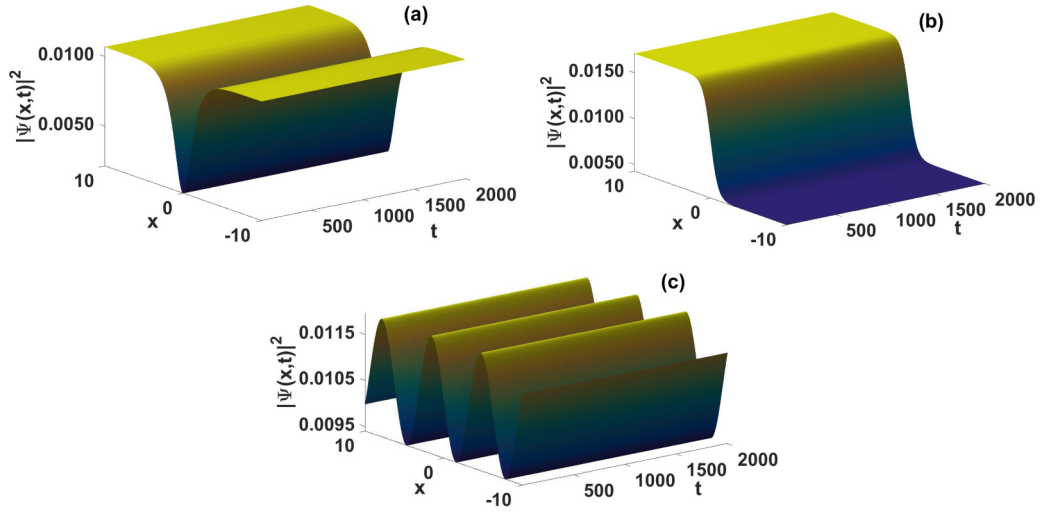

FIG. 7. Profiles changes induced by inhomogeneities as compared to the unperturbed case of Fig. 1(b). (a) Localized inhomogeneity $f(x) = 1 + P_0 \cosh^{-1}(x)$, $P_0 = -0.8$, (b) localized inhomogeneity $f(x) = 1 + R\tanh(x)$, $R = 0.6$, (c) periodic inhomogeneity $f(x) = 1 + P_1 \sin(x)$, $P_1 = 0.12$. $\alpha = 78.92 \times 10^{-12}$ N, and $\chi = 61.76 \times 10^{-12}$ N ($\alpha > \chi$). Other parameters as described in the caption of Fig. 1.

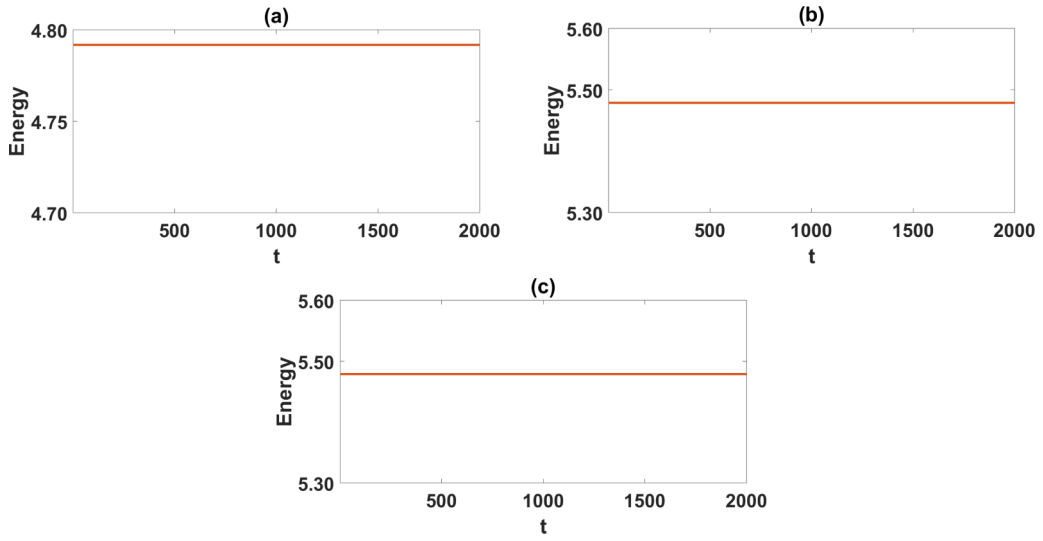

FIG. 8. Energy decreases in the presence of inhomogeneities. (a) Localized inhomogeneity $f(x) = 1 + P_0 \cosh^{-1}(x)$, $P_0 = -0.8$, (b) localized inhomogeneity $f(x) = 1 + R\tanh(x)$, $R = 0.6$, (c) periodic inhomogeneity $f(x) = 1 + P_1 \sin(x)$, $P_1 = 0.12$. $\alpha = 78.92 \times 10^{-12}$ N, and $\chi = 61.76 \times 10^{-12}$ N ($\alpha > \chi$). Other parameters as described in the caption of Fig. 1.

disorder in the smooth functioning of the protein molecular system. The phase of the solutions in Fig. 5 not shown here are identical to the one in Fig. 2(a). We present in Fig. 6 time evolutions of the energies of the solutions in the presence of different types of inhomogeneities. It appears that the periodic inhomogeneity does not affect the energy carried by the waves [see Figs. 6(c) and 3(a)], while the localized inhomogeneities slightly decrease the energies carried by the waves [see Figs. 6(a), 6(b), and 3(a)].

We now turn our attention to the case where $\alpha > \chi$. We draw in Figs. 7 and 8 the spatiotemporal evolutions of the densities and time evolutions of the energies, respectively, of the waves in the presence of inhomogeneities of different types. For the localized inhomogeneity $f(x) = 1 + P_0 \cosh^{-1}(x)$, though the spatiotemporal evolution of the density remains unchanged [see Figs. 7(a) and 1(b)], the energy carried by the wave substantially decreases [see Figs. 8(a) and 3(c)]. The periodic inhomogeneity $f(x) = 1 + P_1 \sin(x)$ and the localized inhomogeneity $f(x) = 1 + R\tanh(x)$ significantly alter the profiles of the waves, but leave energies almost unchanged [see Figs. 8(b), 8(c), and 3(c)]. As stated above, when $f(x) = 1 + R\tanh(x)$ a kink solitary wave is obtained instead of the dark solitary wave of Fig. 1(b) where $f(x) = 1$ [see Figs. 7(b) and 1(b)]. Once again, a periodic profile is obtained for $f(x) = 1 + P_1 \sin(x)$ [see Figs. 7(c) and 1(b)].

It is worth noting that in the above discussions, the off-diagonal parameter and different types of inhomogeneities affect the profiles of the waves as well as the energies they carry. The influence of the strengths of the inhomogeneities have not been analyzed yet. Increasing the strengths of

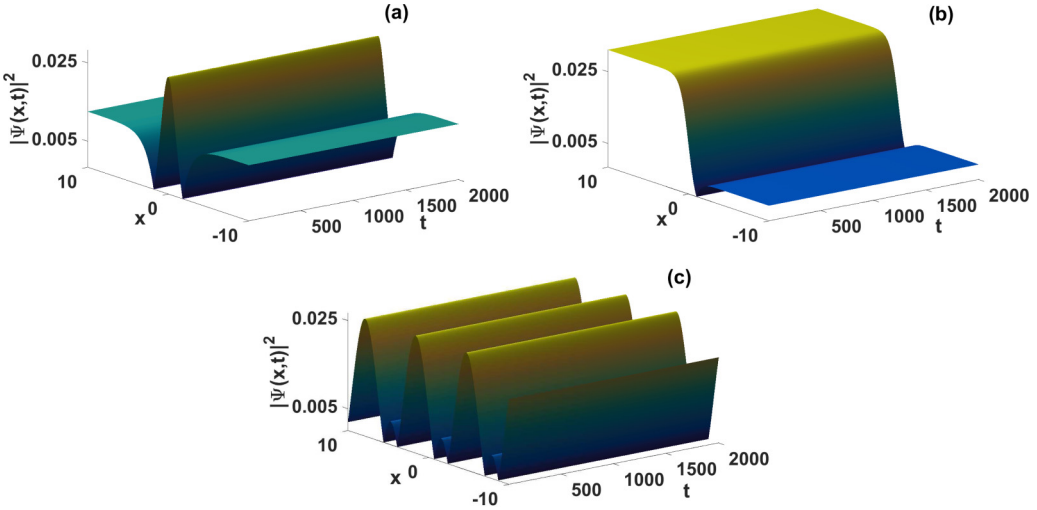

FIG. 9. Large inhomogeneities profoundly change the profiles of solutions as compared to the unperturbed case of Fig. 1(a). (a) Localized inhomogeneity $f(x) = 1 + P_0 \cosh^{-1}(x)$, $P_0 = -8$, (b) localized inhomogeneity $f(x) = 1 + R\tanh(x)$, $R = 3$, (c) periodic inhomogeneity $f(x) = 1 + P_1 \sin(x)$, $P_1 = 5$. $\alpha = 9.92 \times 10^{-12}$ N, and $\chi = 61.76 \times 10^{-12}$ N ($\alpha < \chi$). Other parameters as described in the caption of Fig. 1.

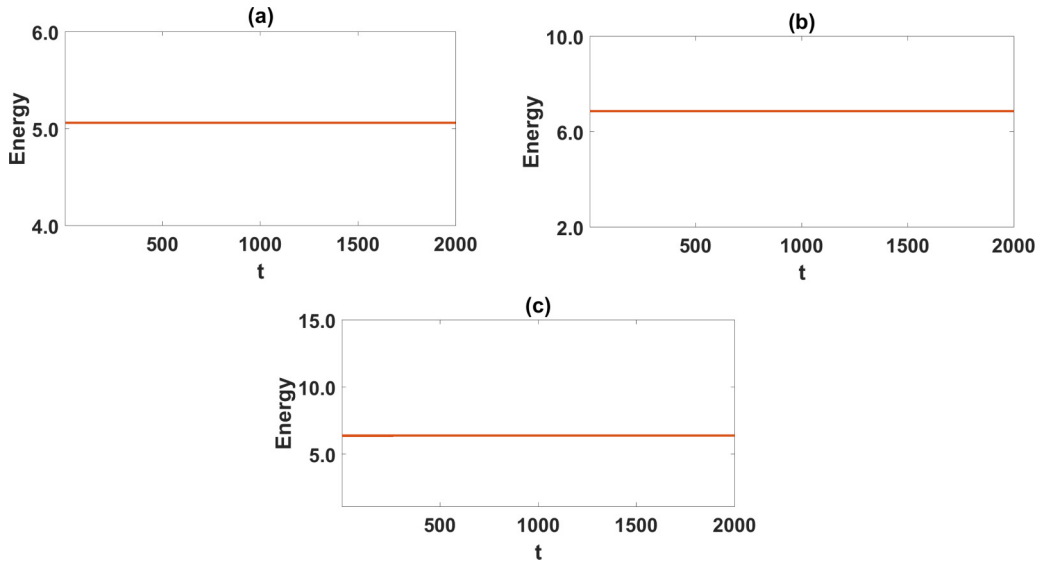

FIG. 10. Substantial increase of energy induced by large inhomogeneities. (a) Localized inhomogeneity $f(x) = 1 + P_0 \cosh^{-1}(x)$, $P_0 = -8$, (b) localized inhomogeneity $f(x) = 1 + R\tanh(x)$, $R = 3$, (c) periodic inhomogeneity $f(x) = 1 + P_1 \sin(x)$, $P_1 = 5$. $\alpha = 9.92 \times 10^{-12}$ N, and $\chi = 61.76 \times 10^{-12}$ N ($\alpha < \chi$). Other parameters as described in the caption of Fig. 1.

the absolute values of the inhomogeneities substantially modify the profiles of the waves in addition to increasing the energies they carry. This can be seen in the spatiotemporal evolutions of densities plotted in Fig. 9 and time variations of energies of Fig. 10. Indeed, a parallel among Figs. 1(a) and 9(a) [$f(x) = 1 + P_0 \cosh^{-1}(x)$, $P_0 = -8$], Fig. 9(b) [$f(x) = 1 + R\tanh(x)$, $R = 3$], and Fig. 9(c) [$f(x) = 1 + P_1 \sin(x)$, $P_1 = 5$], respectively, shows an important change of the profiles accompanied by higher amplitudes induced by large maxima absolute values of inhomogeneities. Furthermore, the energies also increase due to large absolute values of inhomogeneities as confirmed by comparing Fig. 3(a) with Fig. 10(a) [$f(x) = 1 + P_0 \cosh^{-1}(x)$, $P_0 = -8$], Fig. 10(b) [$f(x) = 1 + R\tanh(x)$, $R = 3$], and Fig. 10(c) [$f(x) = 1 + P_1 \sin(x)$, $P_1 = 5$], respectively.

Considering in the case where the absence of inhomogeneities means normal biological functioning of the α-helical protein chains, Figs. 5, 7, and 9 mean that inhomogeneities significantly modify the biological functioning of the proteins which could now be understood as malfunctioning. A similar result was also predicted in Refs. [24,25] where cubic, biquadratic, and periodic inhomogeneities were considered with a bright solitary wave. Conversely, inhomogeneities may be intercalated along the α-helical protein chain at will with high precision. In this case, Figs. 6, 8, and 10 show that the energy propagating through the protein will profoundly increase. Hence, inhomogeneities may be used to amplify the energy transferred through the α-helical protein chain. Such a targeted amplification of energy may be used to treat some diseases.

IV. CONCLUSION

In this work, we have considered a single stranded α-helical protein chain in which the parameter α describes the change in the hopping due to relative transversal displacements of two adjacent amide-I units while the exciton-phonon coupling strength is accounted by the parameter χ. A perturbed nonlinear Schrödinger equation that includes site dependent inhomogeneities has been derived by successive applications of the D2 Ansazt, the continuum limit approximation and the adiabatic approximation. We seek initially the influence of α on the dynamic of the exciton then that of inhomogeneities. Intensive numerical simulations were performed using the fourth-order Runge-Kutta method to search the effects of the model parameters on the dynamic of the exciton propagating through the molecule starting from an hyperbolic initial condition. It appears that, in the absence of inhomogeneities, the interplay between the off-diagonal coupling constant (α) and the diagonal coupling constant (χ) deeply affects the shape of the exciton dynamic propagating through α-helical chains. A stable bright solitary wave is observed when $\alpha < \chi$ while a stable dark solitary wave corresponds to $\alpha > \chi$. Large values of k shrink the width of the waves. The presence of different types of inhomogeneities in single α-helical proteins significantly modifies the profiles of the solitary waves as well as their amplitudes and energies. For relatively small strength inhomogeneities, the bright solitary wave ($\alpha < \chi$) obtained in the absence of inhomogeneities is converted to a dark solitary wave [$f(x) = 1 + P_0 \cosh^{-1}(x)$], a kink solitary wave [$f(x) = 1 + R\tanh(x)$] and a periodic wave [$f(x) = 1 + P_1 \sin(x)$]. For $\alpha > \chi$, the dark solitary wave obtained in the absence of inhomogeneities remains unchanged for $f(x) = 1 + P_0 \cosh^{-1}(x)$ but is transformed to a kink solitary wave [$f(x) = 1 + R\tanh(x)$] and a periodic wave [$f(x) = 1 + P_1 \sin(x)$]. In both cases ($\alpha < \chi$ and $\alpha > \chi$), energies carried by the waves slightly decrease due to the inclusion of inhomogeneities of different types. However, for relatively large values of inhomogeneity strengths, the profiles of the solitary waves are deeply distorted and the energies carried significantly increase. In relation to the biological functioning of the α-helical protein chain, small strength inhomogeneities allow a coherent transport of energy through the molecule under waves of different profiles. This means

that the biological functions are unchanged. Conversely, large strengths of inhomogeneities as they deeply distort the waves, worsen the biological functioning of the molecule. Nevertheless, since the energies significantly increase with large inhomogeneities, the latter may be used to amplify the energy transported through the α-helical protein chain. In such a case, inhomogeneities may be helpful to treat some diseases.

In real life, the α-helix protein is a three-stranded chain molecule. The model used in this work neglects the couplings amount the three chains. Actually, the α-helix structure is a very common feature found in many molecules such as globular proteins (the α-helix structure is predominantly found on the protein surface) and fiber proteins to name just a few. For a better understanding of the whole dynamic, the couplings between the three chains are no longer negligible and must be taken into account in the analysis. The forthcoming work to be carried elsewhere will address the dynamic of a three-stranded chain of proteins in the presence of site dependent inhomogeneities.

[1] L. Pauling, R. B. Corey, and H. R. Branson, Proc. Natl. Acad. Sci. USA **37**, 205 (1951).
[2] G. Abrusan, and J. A. Marsh, PLoS Comput. Biol. **12**, e1005242 (2016).
[3] G. J. Rocklin, T. M. Chidyausiku, I. Goreshnik, A. Ford, S. Houliston, A. Lemak, and D. Baker, Science **357**, 168 (2017).
[4] C. W. F. McClare, Ann. N.Y. Acad. Sci. **227**, 74 (1974).
[5] L. Turin, J. Biol. Phys. **35**, 9 (2009).
[6] A. S. Davydov, J. Theor. Biol. **38**, 559 (1973).
[7] A. S. Davydov, *Solitons in Molecular Systems*, 2nd ed. (Kluwer Academic, Dordrecht, 1991).
[8] A. S. Davydov, Phys. Scr. **20**, 387 (1979).
[9] A. S. Davydov, Physica D **3**, 1 (1981).
[10] A. S. Davydov, Sov. Phys. Usp. **25**, 898 (1982).
[11] A. Scott, Phys. Rep. **217**, 1 (1992).
[12] R. F. Fox, *Biological Energy Transduction* (Wiley, New York, 1982).
[13] V. E. Zakharov and A. B. Shabat, Zh. Éksp. Teor. Fiz. **61**, 118 (1971).
[14] S. Takeno, *Davydov's soliton revisited: Self Trapping of Vibrational Energy in Protein*, edited by P. L. Christeinsen and A. C. Scott (Plenum Press, New York, 1990), NATO ASI Series, vol. 243, p. 31.
[15] A. C. Scott, Phys. Scr. **25**, 651 (1982).
[16] A. C. Scott, Phys. Scr. **29**, 279 (1984).
[17] R. Y. Ondoua, C. B. Tabi, H. P. Ekobena, A. Mohamadou, and T. C. Kofané, Eur. Phys. J. B **85**, 318 (2012).
[18] M. Daniel and M. M. Latha, Physica A **298**, 351 (2001).
[19] M. Daniel and M. M. Latha, Physica A **240**, 526 (1997).
[20] M. Daniel and M. M. Latha, Phys. Lett. A **252**, 92 (1999).
[21] C. B. Tabi, R. Y. Ondoua, H. P. F. Ekobena, and T. C. Kofané, Phys. Lett. A **380**, 2374 (2016).
[22] E. Simo, Phys. Scr. **80**, 045801 (2009).
[23] G. Merlin and M. M. Latha, Physica D **265**, 71 (2013).
[24] S. Saravana Veni, and M. M. Latha, Commun. Nonlin. Sci. Numer. Simul. **19**, 2758 (2014).
[25] A. Mvogo, G. H. Ben-Bolie, and T. C. Kofané, Int. J. Mod. Phys. B **28**, 1450109 (2014).
[26] L. Q. Kong, J. Liu, D. Q. Jin, D. J. Ding, and C. Q. Dai, Nonlinear Dyn. **87**, 83 (2016).
[27] K. Kundu, Phys. Rev. E **61**, 5839 (2000).
[28] X. Pang, S. Chen, X. Wang, and L. Zhong, Int. J. Mol. Sci. **17**, 1130 (2016).
[29] A. J. Heeger, S. Kivelson, J. R. Schrieffer, and W. P. Su, Rev. Mod. Phys. **60**, 781 (1988).
[30] Y. S. Kivshar and M. Peyrard, Phys. Rev. A **46**, 3198 (1992).
[31] D. K. Campbell and A. R. Bishop, *Handbook of Conducting Polymers*, edited by T. A. Skotheim (Marcel Dekker, New York, 1986), vol. 2, p. 937.
[32] C. B Tabi, J. C. Mimshe, H. P. Ekobena, A. Mohamadou, and T. C. Kofané, Eur. Phys. J. B **86**, 374 (2013).
[33] A. S. Davydov, *Solitons in Molecular Systems* (Springer Netherlands, Dordrecht, 1985)
[34] D. Belobo Belobo and T. Meir, Sci. Rep. **8**, 3706 (2018).
[35] D. Belobo Belobo, G. H. Ben-Bolie, and T. C. Kofane, Phys. Rev. E **91**, 042902 (2015).
[36] J. Pouget, M. Remoissenet, and J. M. Tamga, Phys. Rev. B **47**, 14866 (1993).
[37] C. Jin, J. Lumin. **40-41**, 459 (1988).
[38] G. Careri, U. Buontempo, F. Galluzzi, A. C. Scott, E. Gratton, and E. Shyamsunder, Phys. Rev. B **30**, 4689 (1984).
[39] S. Yakada, A. Yaouba, B. Gambo, S. Y. Doka, and T. C. Kofané, Nonlinear Dyn. **87**, 2435 (2017).